Effect of Temperature and Concentration on the Structure of *tert*-Butyl Alcohol/Water Mixtures: Near-Infrared Spectroscopic Study

Dagmara Wojtków and Mirosław A. Czarnecki*

Faculty of Chemistry, University of Wrocław, F. Joliot-Curie 14, 50-383 Wrocław, Poland

Received: May 28, 2005; In Final Form: July 19, 2005

The effect of temperature and concentration on the structure of *tert*-butyl alcohol/water binary mixtures in the alcohol-rich region ($X_{H_2O} < 0.3$) has been studied by using Fourier transform near-infrared (FT-NIR) spectroscopy. The obtained results demonstrate that the addition of a small amount of water to *tert*-butyl alcohol (2-methyl-2-propanol, abbreviated as TBA) leads to minor changes in the structure of neat TBA and suggest that molecules of TBA in the mixture are in the same environment as those in pure TBA. The bands of water are red-shifted in the mixture relative to bulk water, implying that the molecules of water in TBA are involved in stronger hydrogen bonding. The present experimental data give no evidence for the existence of nonbonded water in the mixture. Even at a very low content of water, the main NIR bands of water ($\nu_2 + \nu_3$ and $\nu_1 + \nu_3$) have two components showing markedly different behavior upon an increase in temperature. From the power spectra, it is seen that the extent of intensity changes due to the free OH groups of TBA is smaller in the mixture relative to pure TBA. All of these results support the model of chain-end bonding of water molecules to TBA associates. An increase in X_{H_2O} reduces the population of nonbonded OH groups of TBA, yet both processes do not appear at the same rate. The amount of bonded OH groups of water increases faster than that of the nonbonded ones. It seems that the water−water interaction becomes more important as X_{H_2O} increases. At high alcohol content, the position of the CH alkyl stretching bands is constant, evidencing a negligible role of the hydrophobic hydration in the mixture.

Introduction

Among the monohydroxyl alcohols fully miscible with water in all proportions and at any temperature, *tert*-butyl alcohol (TBA) is the molecule with the largest hydrophobic group. TBA/water mixtures show numerous anomalies in the physicochemical properties and the thermodynamic quantities. Therefore, a great deal of attention has been devoted to the hydration properties of TBA.[1−12] In very diluted solutions, molecules of TBA form hydrogen bonds with molecules of water and they enhance the structure of the water network.[1,2] Above a threshold concentration ($X_{TBA} \approx 0.025-0.03$), the hydrophobic self-association of TBA molecules occurs. The hydrogen/deuterium isotopic substitution neutron diffraction studies demonstrate that the TBA−TBA hydrogen bonds do not appear even at $X_{TBA} = 0.16$.[5] At higher TBA content ($X_{TBA} > 0.2$), the formation of zigzag hydrogen bonding, characteristic for pure TBA, has been postulated.[9] In the TBA-rich region, molecules of water are incorporated into the alcohol structure through hydrogen bonding and each molecule of water acts both as a donor and as an acceptor.[9] In this model, one OH group of water is nonbonded, while the other one is involved in the hydrogen bonding. Koga claims that in concentrated TBA ($X_{TBA} > 0.6$) molecules of water lose the hydrogen-bonded network completely and are dispersed in the TBA liquid structure as single molecules.[1,2] Another model of association in TBA/water mixtures ($X_{TBA} = 0.86$) results from the hydrogen/deuterium isotopic substitution neutron scattering technique and empirical potential structure refinement.[12] The authors prove that at high alcohol content the molecules of water tend to associate in small hydrogen-bonded clusters of two or three molecules around a center situated on a water oxygen atom. Each of these models predicts a different pattern of the spectra in the region of water absorption. Thus, it seems that a close examination of the vibrational spectra should indicate the most relevant model.

Studies of alcohol/water mixtures were predominantly performed in the water-rich region, whereas few experimental attempts have been undertaken in the alcohol-rich region. As a result, the aggregation process has been studied by looking at the behavior of water molecules rather than that of alcohol ones. This is the next paper in the series on studies of interactions between alcohols and water in the alcohol-rich region.[13] The present work is focused on the effect of temperature and concentration on the structure of TBA/water mixtures. An application of Fourier transform near-infrared (FT-NIR) spectroscopy together with 2D correlation analysis and chemometric methods permitted us to explore the subtle changes in the liquid alcohol structure caused by the presence of water as well as the state of water in the mixture. We direct particular attention to comparison of the present results with those published for butan-1-ol/water mixtures (butan-1-ol abbreviated as NBA).[13] Our studies on NBA/water mixtures in the alcohol-rich region suggest the presence of two different species of hydrogen-bonded water.[13] In addition, we have postulated the existence of molecules of water not involved in hydrogen bonding. Our results reveal that in NBA/water mixtures alcohol−alcohol and water−water interactions dominate, whereas the water−alcohol interaction is weaker.[13] As a result, NBA is only partially miscible with water. The properties of TBA/water mixtures are different from those of *n*-alcohols, and hence, one can expect

* To whom correspondence should be addressed. Fax: 48-71-3282348. E-mail: mcza@wchuwr.chem.uni.wroc.pl.

10.1021/jp052833n CCC: $30.25
Published on Web 08/20/2005

that these differences will be manifested in the vibrational spectra.

Experimental Section

TBA (99.8%) was purchased from Aldrich Chemical Co. (Germany) and was used as received. High-purity water (resistivity 18.2 MΩ·cm) was obtained by the Simplicity 185 Ultrapure Water System (Milliphore Corporation). Samples of TBA/water were prepared by weight. FT-NIR spectra were recorded at a resolution of 4 cm^{-1} on a Nicolet Magna 860 spectrometer with a DTGS detector, and 512 scans were accumulated. The sample chamber was purged with dry nitrogen. The spectra of the mixture were measured in a variable-temperature quartz cell (Hellma) of 5 mm thickness from 30 to 75 °C. A few series of the concentration-dependent spectra with X_{H_2O} from 0.001 to 0.3 were recorded in the same cell at 30 °C.

2D Correlation Analysis. Prior to 2D correlation analysis, the spectra were corrected for the density change with temperature and then the baseline fluctuations were minimized by an offset at 9000 cm^{-1}. The dynamic spectrum $\mathbf{A}^d(\nu,t)$ was created by subtraction of a reference spectrum from an ordered series of the experimental spectra $\mathbf{A}(\nu,t)$. Here, ν represents the spectral variable, whereas t represents the temperature or concentration. The spectrum of pure TBA at 30 °C and an average spectrum were used as references for the concentration- and temperature-dependent data, respectively. The discrete synchronous $\Phi(\nu_1,\nu_2)$ and asynchronous $\Psi(\nu_1,\nu_2)$ 2D correlation intensity determined at N equally spaced points were calculated as follows[14,15]

$$\Phi(\nu_1,\nu_2) = \frac{1}{N-1}\mathbf{A}^d(\nu_1,t)\cdot\mathbf{A}^d(t,\nu_2) \quad (1)$$

$$\Psi(\nu_1,\nu_2) = \frac{1}{N-1}\mathbf{A}^d(\nu_1,t)\cdot\mathbf{M}\cdot\mathbf{A}^d(t,\nu_2) \quad (2)$$

For $j,k = 1, 2, \ldots, N$, the Hilbert−Noda transformation matrix $\mathbf{M}$ is given by

$$\mathbf{M} = \begin{cases} 0 & \text{if } j = k \\ 1/\pi(k-j) & \text{otherwise} \end{cases} \quad (3)$$

A positive synchronous peak at ν_1/ν_2 indicates that the intensity changes at these two wavenumbers are in the same direction. The asynchronous spectra were multiplied by a sign of the companion synchronous spectra. Thus, a positive asynchronous cross-peak at ν_1/ν_2 implies that the spectral change at ν_1 occurs faster (earlier) than that at ν_2. Negative synchronous and asynchronous peaks indicate the opposite.

The synchronous spectrum yields information on the similarity of the spectral changes at ν_1 and ν_2 during the period from t_{min} to t_{max}. A synchronous spectrum is symmetric with respect to a diagonal, and the peaks along the diagonal are called autopeaks. The autopeaks represent the overall extent of the spectral changes at particular wavenumbers. Namely, regions of the dynamic spectrum that significantly vary the intensity will develop strong autopeaks. The diagonal of the synchronous spectrum is called the power spectrum. The cross-peaks represent simultaneous variation of the spectral intensities at two different wavenumbers, ν_1 and ν_2. The autopeaks are always positive, while the sign of the cross-peaks can be either positive or negative. The existence of a cross-peak at ν_1/ν_2 indicates the possibility that the bands at ν_1 and ν_2 originate from the same fragment of the molecule or two different fragments strongly interacting. In contrast, the asynchronous spectrum $\Psi(\nu_1,\nu_2)$ provides information on how much the features at ν_1 and ν_2 are dissimilar to each other during the period from t_{min} to t_{max}. An asynchronous spectrum is antisymmetric with respect to the diagonal and consists exclusively of the cross-peaks. The sign of the asynchronous cross-peaks can be either positive or negative. The asynchronous spectrum develops a peak at ν_1/ν_2 if the spectral changes at ν_1 and ν_2 vary out of phase at least for some values of perturbation from the range of $\langle t_{min},t_{max}\rangle$. This property is very helpful in resolving highly overlapped peaks. As long as the responses at ν_1 and ν_2 are different, the corresponding bands are resolved in the asynchronous spectrum, regardless of the separation between the original peaks. One has to stress that the synchronous peaks only indicate the possibility of the presence of the correlation between various bands. On the other hand, the asynchronous peaks resolve the bands responding at different rates with a high level of certainty. Due to the symmetry properties, it is enough to take into account only one-half of the synchronous (asynchronous) spectrum. The 2D correlation analysis was performed using MATLAB 6.5 (The Math Works Inc.) based software written in our laboratory (synasyn.m).

Chemometric Analysis. The spectral data form a matrix $\mathbf{D}$ of size $N \times M$, where N is the number of spectra with different values of X_{H_2O} and M is the number of data points in each spectrum. The matrix $\mathbf{D}$ is obtained from the matrix $\mathbf{A}$ as follows

$$\mathbf{D} = \mathbf{A}/b \quad (4)$$

where b is the optical path length. Assuming an additivity of the spectra, one can decompose the matrix $\mathbf{D}$ as a product of the concentration profile matrix ($\mathbf{C}$) and the matrix of pure component spectra ($\mathbf{S}^T$).

$$\mathbf{D} = \mathbf{C}\mathbf{S}^T + \mathbf{E} \quad (5)$$

where $\mathbf{E}$ is the matrix of residuals that takes into account the random variation of $\mathbf{D}$ and therefore does not include any significant information. The successful resolution of $\mathbf{D}$ into pure component spectra and spectral profiles depends on the ability of correct determination of the number of significant species present in the system (K). In the absence of noise and baseline fluctuations, K is equal to the chemical rank of $\mathbf{D}$. The chemical rank means the number of variables necessary to reconstruct the data matrix within the noise level. The value of K was estimated by principal component analysis (PCA)[16] and then confirmed by a cross-validation procedure[17] and evolving factor analysis (EFA).[18]

PCA finds a combination of variables that describe major trends in the data by decomposing the data matrix $\mathbf{D}$ as a sum of the outer product of vectors t_i (scores) and p_i (loadings) plus a residual matrix $\mathbf{E}$:

$$\mathbf{D} = \mathbf{T}\mathbf{P}^T + \mathbf{E} = \sum_{i=1}^{K} t_i p_i^T + \mathbf{E} \quad (6)$$

The score matrix and the loading matrix can be regarded as abstract representations of the actual concentration and spectral profiles, respectively. Scores contain information on how the samples relate to each other, whereas loadings contain information on how the variables relate to each other. When determining the number of PCs, it is useful to list the eigenvalues in a table along with the percentage of the variance that each PC captures. During inspection of these values, one looks for a sudden jump in the values. The eigenvalues of the significant chemical components should be larger than those due to the noise and

baseline fluctuations. One can obtain the latter value from the analysis in the nonabsorbing region of the spectrum. It can also be helpful to look at the plots of the scores and loadings. When the scores or loadings become random, it is probable that they are capturing nondeterministic variation. It is also possible to choose the number of PCs on the basis of EFA.[18] The fundamental idea of EFA is to follow the singular values of a data matrix as rows (samples) are added. Once the singular values are determined, they can be plotted against the ordered variable. As new factors enter the data, new significant singular values will rise from the baseline of small singular values due to the presence of noise in the data.

However, the actual concentration profiles and pure component spectra cannot be obtained directly from principal components decomposition of **D** without additional information because the equation

$$\mathbf{D}_{\text{est}} = \mathbf{TP}^{\text{T}} = \mathbf{TRR}^{-1}\mathbf{P}^{\text{T}} = \mathbf{CS}^{\text{T}} \tag{7}$$

has an infinite number of solutions for an arbitrary invertible transformation matrix **R**. This ambiguity is delimited if the constraints are imposed on the resolution process. The concentration profiles and the pure component spectra were obtained by the multivariate curve resolution (MCR) approach with constraints.[19,20] This is an iterative method that calculates in each cycle a new **C** and **S** in such a way that the matrix **E** is minimized. The concentration profiles obtained from EFA are used as initial estimates in the constrained and alternating least squares optimization. The spectral profiles are obtained as

$$\mathbf{S}^{\text{T}} = (\mathbf{C}^{\text{T}}\mathbf{C})^{-1}\mathbf{C}^{\text{T}}\mathbf{D} \tag{8}$$

Next, the spectral profiles can be used to determine the pure concentration profiles by least squares as

$$\mathbf{C} = \mathbf{DS}(\mathbf{S}^{\text{T}}\mathbf{S})^{-1} \tag{9}$$

The matrices **C** and **S** include a set of constraints that reflect our knowledge on the studied system. One of the commonly used assumptions is that both concentrations and spectra are non-negative. Using this constraint, it is often possible to extract the values of **C** and **S** through a procedure of least squares optimization. The chemometric analysis was performed by PLS-Toolbox 3.0 (Eigenvector Research Incorporated) for use with MATLAB.

Results and Discussion

Effect of Temperature on Spectra of Pure TBA. 2D correlation spectra of pure TBA have already been published,[21] yet the assignments of some bands should be revisited. Figure 1A shows the effect of temperature on FT-NIR spectra of pure TBA. Corresponding synchronous and asynchronous spectra (not shown) are similar to those presented in ref 21 (Figure 6). Assignments of major spectral features appearing in this region are collected in Table 1. In previous papers, the band near 6850 cm^{-1} was assigned to the cyclic dimers.[21−23] As discussed in detail, the cyclic dimer is a transition species rather than a stable form, and therefore, this band should be assigned to the linear dimer.[24] The high-frequency components of the "polymer" band near 6500 cm^{-1} (Figure 8 in ref 21) were attributed to different hydrogen-bonded species. However, in this spectral region occurs a series of ν(CH) + ν(OH) combination bands involving the free OH groups.[23−25] Thus, the shape of the polymer band is a result of overlapping with the combination band.

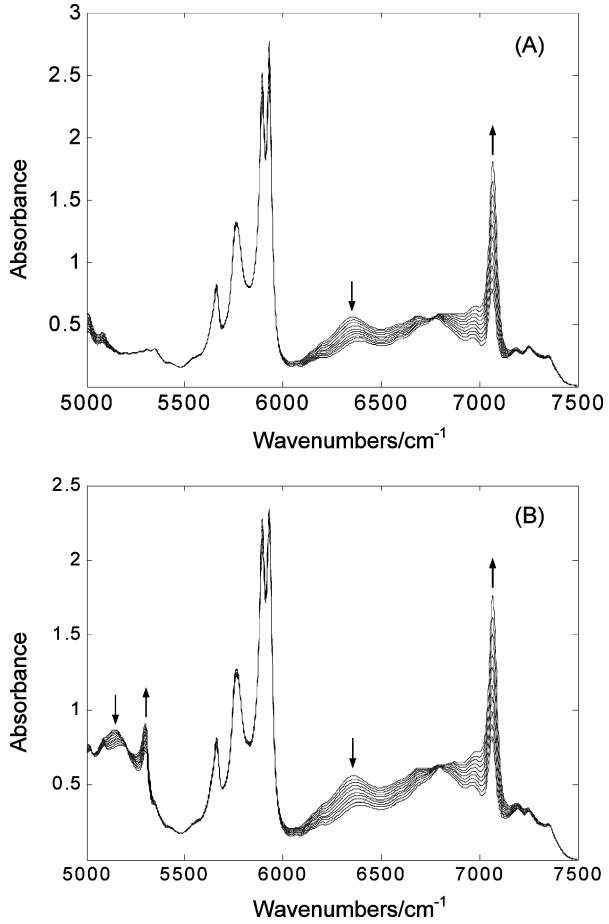

Figure 1. FT-IR spectra of pure TBA (A) and the TBA/water mixture with $X_{H_2O} = 0.1$ (B) from 30 to 75 °C. The arrows indicate the direction of intensity changes as the temperature is increased.

TABLE 1: Frequencies and Assignments of Selected NIR Bands of Pure TBA, Pure Water, and TBA/Water Mixtures

position (cm^{-1})	vibration	species	molecule
5155	$\nu_2 + \nu_3$	associated	water
5183	$\nu_2 + \nu_3$	associated	water[a]
5300	$\nu_2 + \nu_3$	free (one-bonded)	water
5893, 5928	2ν(CH)		TBA
6327	2ν(OH)	higher multimers	TBA
6873	$\nu_1 + \nu_3$	associated	water
6879 → 6892[b]	2ν(OH)	dimer	TBA
6898	$\nu_1 + \nu_3$	associated	water[a]
6981	2ν(CH) + δ(CH)		TBA
7060	2ν(OH)	free (end-chain)	TBA
7070	2ν(OH)	free	TBA
7186, 7251	2ν(CH) + δ(CH)		TBA
7207	$\nu_1 + \nu_3$	free (one-bonded)	water
8426	3ν(CH)		TBA

[a] Pure water at 30 °C. [b] 6879, pure TBA; 6892, TBA/water (X_{H_2O} = 0.1).

The high-resolution nuclear magnetic resonance study has shown that the structure of liquid TBA is dominated by cyclic species (mostly tetramers).[26] Increasing temperature tends to reduce the extent of hydrogen bonding in liquid TBA and shifts the equilibrium toward creation of the monomers and linear associates. The chains of TBA are relatively short because of steric interactions.[27] The temperature-induced transition from rings to chains corresponds to a relatively large increase in the number of nonbonded OH groups in the system. Among intermediate species, the linear dimers seem to play a special role, since the dimer band (near 6850 cm^{-1}) appears in the 2D correlation spectra of all studies of alcohols.[21−24,28−30]

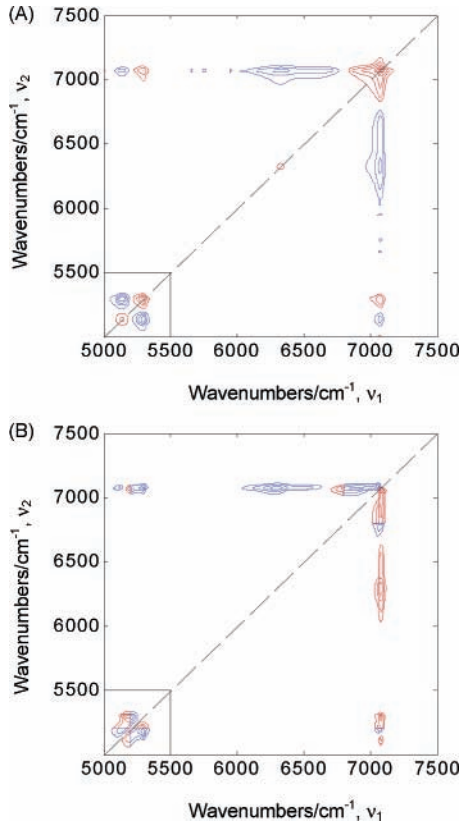

Figure 2. (A) Synchronous and (B) asynchronous spectra of the TBA/water mixture ($X_{H_2O} = 0.1$) from 30 to 75 °C. The red lines represent positive correlation peaks, whereas the blue lines represent negative peaks. The intensities in the 5000−5500 cm^{-1} range were enlarged to appear in this scale.

Effect of Temperature on Spectra of the TBA/Water Mixture. Figure 1B shows FT-NIR spectra of the TBA/water mixture ($X_{H_2O} = 0.1$) from 30 to 75 °C. As compared with the spectra of pure TBA (Figure 1A), the most important differences occur below 5500 cm^{-1}. In this region is located the $\nu_2 + \nu_3$ band of water that has two components. The low-frequency component (near 5155 cm^{-1}) decreases in intensity and shifts to higher wavenumbers as the temperature increases. In going from 30 to 75 °C, this shift is about 30 cm^{-1}. The other band (at 5300 cm^{-1}) increases in intensity and does not vary in position. The analogous band for the NBA/water mixture was assigned to nonbonded molecules of water dispersed among hydrocarbon chains of the alcohol.[13] However, this band can be assigned to one-bonded water as well. The existence of one-bonded water was evidenced in solutions of water with some organic compounds in *n*-heptane.[31] Figure 2 shows the synchronous and asynchronous spectra constructed from the data presented in Figure 1B. As can be seen, above 6000 cm^{-1}, the spectrum is very similar to that of pure TBA (Figure 6 in ref 21), suggesting that in the alcohol-rich region the structure of TBA is not perturbed by the addition of water.[13,32−34] The pattern of asynchronous intensity in the 5000−5500 cm^{-1} region (Figure 2) is characteristic of a shifting band.[35−37] However, the higher-frequency component of the water band and the band due to nonbonded OH groups of TBA do not shift, and therefore, the asynchronous intensity between these peaks (at 5300/7070 cm^{-1}) has a physical meaning. From the sign of this peak, it is seen that the population of nonbonded OH groups increases faster for TBA than that for water. It has been suggested that in the alcohol-rich region the molecules of water are bonded to the chain-end molecules of alcohol that act preferentially as hydrogen-bond acceptors.[32,38] In this model, one OH group of water is bonded to the alcohol, whereas the second one is nonbonded. Thus, for each band of water, one can expect two components. Indeed, this conclusion agrees with the experimental data (Figure 1B).

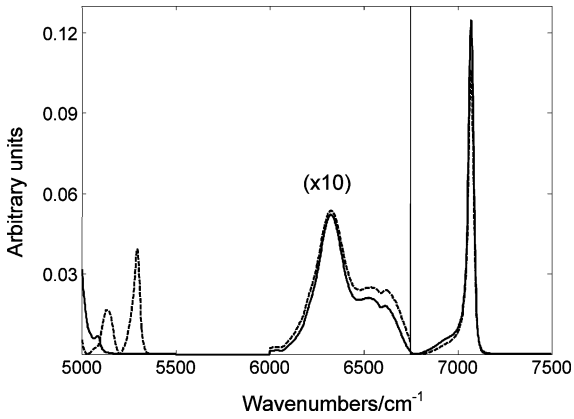

Figure 3. Power spectra obtained from the synchronous spectra of pure TBA (solid line) and the TBA/water mixture with $X_{H_2O} = 0.1$ (dashed line).

As shown, during the thermal breaking of hydrogen-bonded alcohols, the terminal molecules are removed at first.[24] At $X_{H_2O} = 0.1$, the population of molecules of water is not sufficient to occupy all chain-end positions, and thus, the mechanism of hydrogen-bonding destruction in the TBA/water mixture is similar to that in bulk TBA. However, comparison of the power spectra displayed in Figure 3 reveals that an extent of intensity changes due to the free OH groups of TBA drops in going from bulk TBA to the mixture. This is in agreement with the model of the chain-end bonding of molecules of water to TBA associates, since this process reduces the number of the terminal molecules of TBA. In contrast, the power spectra of NBA and the NBA/water mixture (Figure 6 in ref 13) prove that the addition of water to NBA results in faster increase in the population of the free OH groups of the alcohol. Hence, one can conclude that the associates of NBA are broken more easily in the presence of water.

Effect of X_{H_2O} on Spectra of the TBA/Water Mixture. Figure 4A shows the synchronous spectrum of the TBA/water mixture at 30 °C with X_{H_2O} from 0.1 to 0.3 constructed from the difference spectra. The difference spectra were calculated by subtraction of the spectrum of pure TBA at 30 °C from each of the mixture spectra. The most prominent changes occur in the region of water absorption (near 5150, 5300, and 6900 cm^{-1}), while the bands of TBA (near 6300 and 7070 cm^{-1}) do not seem to vary in intensity. All synchronous peaks are positive, showing that an increase in X_{H_2O} leads to the growth of the intensities of the water bands. Figure 4B displays the power spectrum obtained from the synchronous spectrum shown in Figure 4A. Evidently, the bands due to the absorption of water have two components. The more intense and broad band was assigned to the bonded water, whereas a narrow peak at higher frequency was attributed to the free OH groups of water. An examination of Figure 4B reveals a sharp drop in intensity at the position of the "monomer" band of TBA (near 7070 cm^{-1}). This effect results from the overlap of two bands changing intensity in the opposite direction, and a similar phenomenon was observed in the power spectra of other alcohols.[23,24] Hence, one can conclude that an increase in X_{H_2O} reduces the population of the nonbonded OH groups of TBA.

The major part of intensity variations in concentration-dependent spectra originates from the changes in concentration

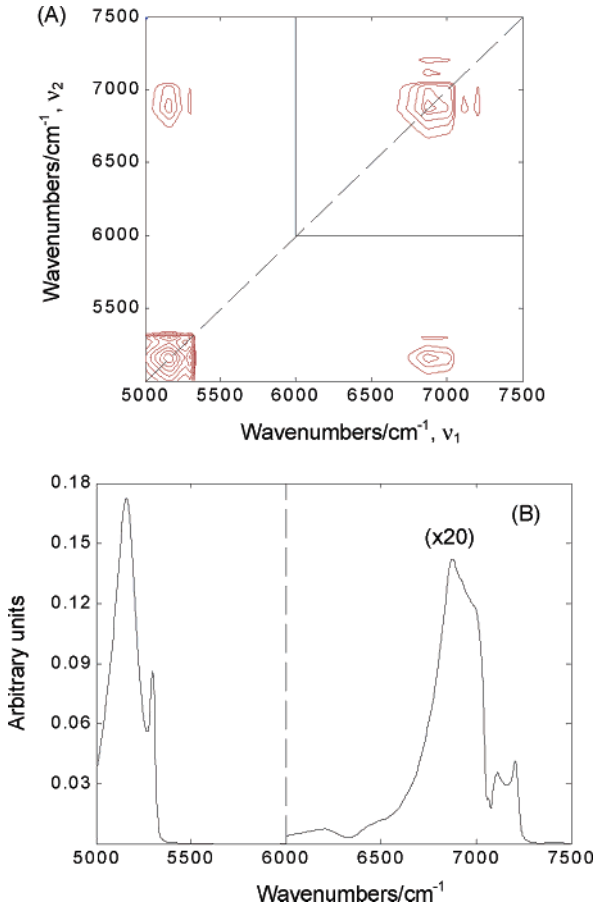

Figure 4. (A) Synchronous spectrum of the TBA/water mixture constructed from the concentration-dependent spectra with X_{H_2O} from 0.16 to 0.3. The red lines represent positive correlation peaks, whereas the blue lines represent negative peaks. (B) Corresponding power spectrum. The intensities in the 6000−7500 cm^{-1} range were enlarged to appear in this scale.

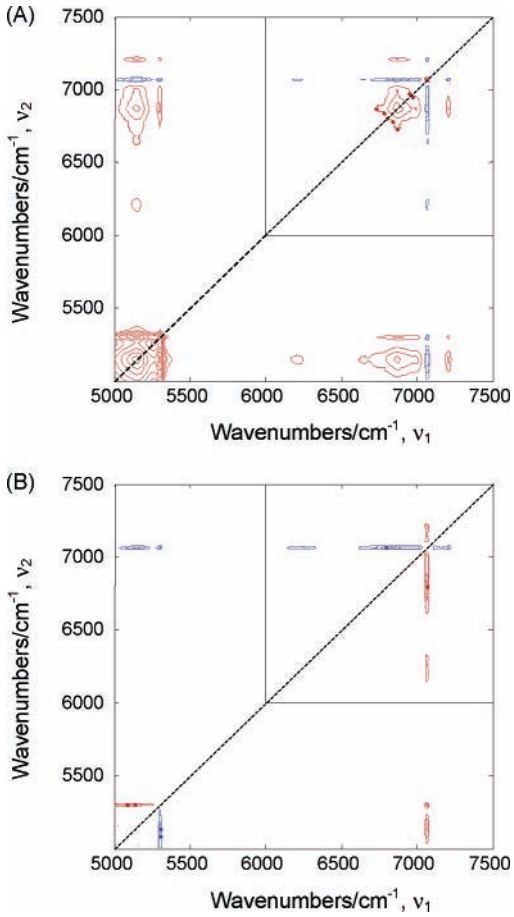

Figure 5. (A) Synchronous and (B) asynchronous spectra of TBA/water mixtures with X_{H_2O} from 0.16 to 0.3 at 30 °C. The spectra were constructed from the concentration-normalized data. The red lines represent positive correlation peaks, whereas the blue lines represent negative peaks. The intensities in the 6000−7500 cm^{-1} range were enlarged to appear in this scale.

itself. To eliminate this effect and obtain asynchronous intensity with physical meaning, at first, the difference spectra should be concentration-normalized.[39] Figure 5 shows 2D correlation spectra constructed from the normalized data. The positive synchronous cross-peaks (Figure 5A) occur between the bands assigned to water, whereas a clear negative intensity appears between the monomer band of TBA and the other peaks. This is direct evidence that the population of the free OH groups of TBA is reduced when X_{H_2O} increases. In contrast, the population of the higher multimers of TBA shows an opposite trend (positive synchronous peak at 5155/6300 cm^{-1}). The position of the original peaks does not depend on X_{H_2O}, and hence, the asynchronous intensity in Figure 5B is a real one. The presence of series of asynchronous peaks at 7070 cm^{-1} means that an increase in X_{H_2O} and a decrease in the population of the free OH groups of TBA do not appear at the same rate. From the sign of the asynchronous peak at 5155/5300 cm^{-1} (Figure 5B), one can conclude that the population of bonded OH groups of water increases faster relative to the nonbonded ones. At low to moderate X_{H_2O}, the molecules of water form a one-bonded complex with the free terminal OH groups of TBA. Thus, the populations of the free and bonded OH groups of water increase at the same rate and the asynchronous spectra obtained from the concentration-normalized spectra with a small content of water ($X_{H_2O} < 0.1$) do not develop significant peaks (not shown). At higher values of X_{H_2O}, the water−water interactions become more important and as a result the population of bonded OH groups of water increases faster as compared with the nonbonded groups.

Numerous papers prove that an increase in the molar fraction of alcohol in the water-rich region is accompanied by a significant shift (4−8 cm^{-1}) in the fundamental frequencies of the symmetric and antisymmetric alkyl stretching bands.[4,8,32,40] At high alcohol content, the rate of the changes is minimal, indicating little or no hydrocarbon chain−water contact.[4,40] An examination of all measured spectra of TBA/water mixtures does not reveal any shift in the position of the alkyl stretching bands up to $X_{H_2O} = 0.3$. Hence, one can conclude that in the alcohol-rich region the hydrophobic hydration is negligible.

Chemometric Analysis of TBA/Water Mixtures. PCA was performed on the spectra of TBA/water mixtures with X_{H_2O} from 0.01 to 0.1. Table 2 shows the eigenvalues and captured variance for all principal components. As can be seen, the first two principal components explain 99.99% of the variance in the data. The score plot for the third PC (and higher) has a random character (not shown). The corresponding loading plot also does not include any significant information. Finally, the residual matrix left after the removal of two eigenvectors is small and reveals mainly random variance. Thus, the results of PCA suggest the presence of two species in the mixture of TBA/water. In Figure 6 are displayed the results of EFA of the same data. The dotted line indicates the level of noise estimated from the nonabsorbing region of the spectrum (7600−8100 cm^{-1}).

TABLE 2: Percent Variance Captured by the PCA Model[a]

		% variance captured	
principal component	eigenvalue	this PC	total
1	4.70e+002	99.29	99.29
2	3.31e+000	0.70	99.99
3	4.00e−002	0.01	100.00
4	2.65e−003	0.00	100.00
5	6.13e−004	0.00	100.00
6	2.57e−004	0.00	100.00
7	1.58e−004	0.00	100.00
8	3.50e−005	0.00	100.00
9	2.81e−005	0.00	100.00
10	1.48e−005	0.00	100.00

[a] The PCA was performed on the data matrix of TBA/water mixtures with X_{H_2O} from 0.01 to 0.1 in the range 5000−7500 cm^{-1}.

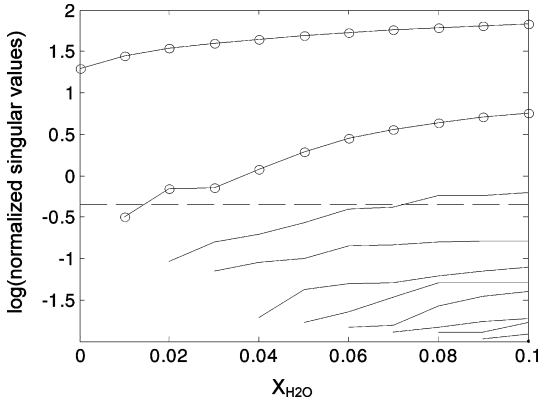

Figure 6. EFA of TBA/water mixtures with X_{H_2O} from 0.01 to 0.1. The dashed line represents the estimated noise level.

Also, this result suggests that experimental data contain two significant eigenvectors.

The concentration profiles obtained from EFA (the lines with the circles in Figure 6) were used as initial estimates in the MCR procedure with constraints (non-negativity on concentration and spectra). The unique resolution of multicomponent systems into pure spectra and concentration profiles can be performed if selective regions of the spectra can be found for all of the significant components.[19,20] Interestingly, taking the initial estimates of the concentration profiles from the selective regions (at 5150 and 6300 cm^{-1}), we obtained exactly the same results as those starting from EFA results. On the other hand, the trials of resolving of the three components did not succeed regardless of the method of estimation of the concentration profiles. In Figure 7A are displayed the spectral profiles obtained from MCR of TBA/water mixtures with X_{H_2O} from 0.01 to 0.1. One of these profiles can be assigned to TBA, whereas the second one represents the changes due to water. The similarity between the spectral profile of TBA and the spectrum of pure TBA (Figure 1A) suggests that molecules of TBA in the mixture are in the same environment as those in bulk alcohol. This confirms the conclusion derived from 2D correlation analysis and agrees with numerous literature reports.[4,8,10,33,34,40] In contrast, the spectral profile of water obtained from the MCR procedure differs from the spectrum of bulk water (Figure 7). Like in the case of the NBA/water mixture,[13] the main bands of water ($\nu_2 + \nu_3$ and $\nu_1 + \nu_3$) have high-frequency components. The position and relatively small half width of these additional bands indicate the presence of the free OH groups in nonbonded or singly bonded water. The existence of nonbonded water in TBA/water mixtures at high alcohol content has been suggested by Koga.[2] However, even at a very low content of water (X_{H_2O} = 0.002), the water band has two components (Figure 8). This

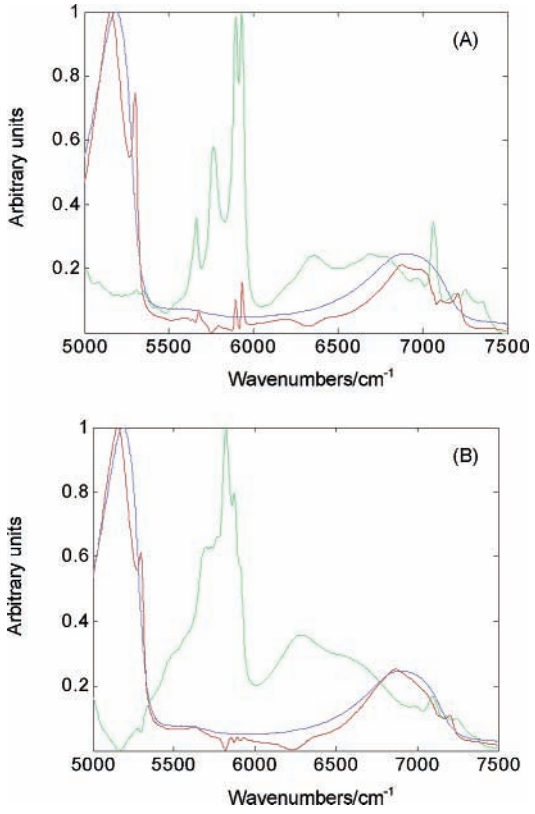

Figure 7. Spectral profiles obtained from MCR of TBA/water (A) and NBA/water (B) mixtures with X_{H_2O} from 0.01 to 0.1. The green lines represent the spectral profiles of the alcohols, the red lines represent the profiles of water, and the spectrum of pure water at 30 °C is displayed in blue. All spectra were normalized to unity absorbance.

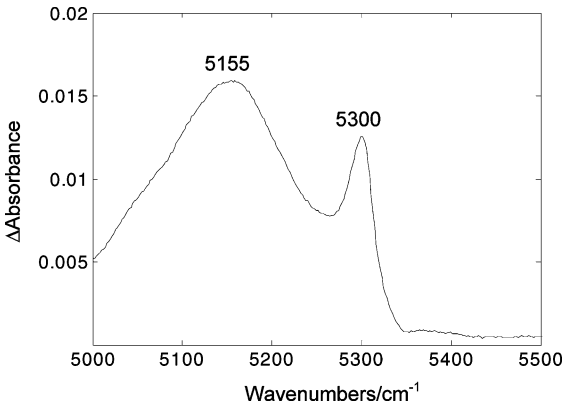

Figure 8. Difference spectrum obtained by subtraction of the spectrum of pure TBA from the spectrum of the mixture with X_{H_2O} = 0.002.

observation rather excludes the presence of nonbonded water in the mixture. In going from bulk water to the mixture, these bands are red-shifted, showing that the molecules of water are more strongly bonded in the mixture. The spectral profiles of water (Figure 7A) are narrower in the mixture, suggesting that the movement of molecules of water is more restricted in TBA as compared with the bulk water. This observation agrees with the other literature reports.[4,41]

Figure 7B shows the spectral profiles obtained from MCR of NBA/water mixtures with X_{H_2O} from 0.01 to 0.1. The profile of NBA is similar to the spectrum of bulk NBA (Figure 5 in ref 21). As can be seen, the monomer peak of NBA (near 7100 cm^{-1}) is noticeably weaker relative to the polymer peak (near 6250 cm^{-1}). This contrasts with the results obtained for TBA (Figure 7A). Evidently, the self-association is more favored in

NBA.[21,42] It is of interest that the intensity of the peak due to nonbonded OH groups of water (at 5300 cm^{-1}) is significantly higher in TBA/water mixtures than that in NBA/water mixtures (Figure 7). Thus, in the latter case, the population of one-bonded water is smaller. The majority of molecules of water form two bonds (or more) predominantly to other molecules of water. As shown, the NBA−water interactions are weaker than the water−water interactions. [13] It appears that the molecules of water in NBA tend to associate in small hydrogen-bonded clusters,[12] whereas in TBA solution dominates the chain-end association. Probably, this is a main reason for the observed differences in the properties of aqueous solutions of both alcohols.

Conclusions

The present work provides a systematic study of the effect of temperature and concentration on the structure of TBA/water mixtures in the alcohol-rich region ($X_{H_2O} < 0.3$). An increase in X_{H_2O} leads to a decrease in the population of nonbonded OH groups in TBA, evidencing that the molecules of water are attached mainly to the chain-end OH groups of TBA. From the shape of the water spectrum obtained from MCR, one can conclude that the interaction of TBA and water is stronger than that in bulk water. Further, the movement of the molecules of water is more restricted in the mixture relative to bulk water. The bands due to water have two components even at a very low content of water; hence, it excludes the presence of the free molecules of water in the mixture. The low-frequency band near 5155 cm^{-1} was assigned to OH groups of water bonded to chain-end TBA, while the high-frequency band at 5300 cm^{-1} was assigned to the free OH groups in one-bonded water. The results of both 2D correlation and chemometric analysis evidence that the structure of TBA in the mixture is the same as that in the pure liquid TBA. The constant position of the methyl stretching bands indicates that the hydrophobic interactions in this concentration range are negligible. On the contrary to NBA, in going from pure TBA to the mixture, one can observe a drop in the extent of intensity changes due to the free OH groups of the alcohol. This finding is consistent with the chain-end mechanism of the association of water in TBA.

Acknowledgment. The authors gratefully acknowledge Bogusława Czarnik-Matusewicz (University of Wrocław) for helpful discussion and providing the spectra of pure water.

References and Notes

(1) Koga, Y. *Can. J. Chem.* **1988**, *66*, 1187.
(2) Koga, Y. *Can. J. Chem.* **1988**, *66*, 3171.
(3) Nishikawa, K.; Iijima, T. *J. Phys. Chem.* **1990**, *94*, 6227.
(4) Onori, G.; Santucci, A. *J. Mol. Liq.* **1996**, *69*, 161.
(5) Bowron, D. T.; Finney, J. L.; Soper, A. K. *J. Phys. Chem. B* **1998**, *102*, 3551.
(6) Mayele, M.; Holz, M.; Sacco, A. *Phys. Chem. Chem. Phys.* **1999**, *1*, 4615.
(7) Mizuno, K.; Kimura, Y.; Morichika, H.; Nishimura, Y.; Shimada, S.; Maeda, S.; Imafuji. S.; Ochi, T. *J. Mol. Liq.* **2000**, *85*, 139.
(8) Freda, M.; Onori, G.; Santucci, A. *J. Phys. Chem. B* **2001**, *105*, 12714.
(9) Yoshida, K.; Yamaguchi, T.; Kovalenko, A.; Hirata, F. *J. Phys. Chem. B* **2002**, *106*, 5042.
(10) Freda, M.; Onori, G.; Santucci, A. *Phys. Chem. Chem. Phys.* **2002**, *4*, 4979.
(11) Michele, A.; Freda, M.; Onori, G.; Santucci, A. *J. Phys. Chem. A* **2004**, *108*, 6145.
(12) Bowron, D. T.; Moreno, S. D. *J. Phys.: Condens. Matter* **2003**, *15*, 121.
(13) Czarnecki, M. A.; Wojtków, D. *J. Phys. Chem. A* **2004**, *108*, 2411.
(14) Noda, I. *Appl. Spectrosc.* **1993**, *47*, 1329.
(15) Noda, I. *Appl. Spectrosc.* **2000**, *54*, 994.
(16) Wold, S.; Esbensen, K.; Geladi, P. *Chemom. Intell. Lab. Syst.* **1987**, *2*, 37.
(17) Wise, B. M.; Ricker, N. L. *J. Chemom.* **1993**, *7*, 1.
(18) Keller, H. R.; Massart, D. L. *Chemom. Intell. Lab. Syst.* **1992**, *12*, 209.
(19) Tauler, R.; Kowalski, B. *Anal. Chem.* **1993**, *65*, 2040.
(20) Tauler, R.; Izquiedoro-Ridorsa, A.; Casassas, E. *Chemom. Intell. Lab. Syst.* **1993**, *18*, 293.
(21) Czarnecki, M. A.; Maeda, M.; Ozaki, Y.; Suzuki, M.; Iwahashi, M. *J. Phys. Chem. A* **1998**, *102*, 9117.
(22) Czarnecki, M. A.; Maeda, H.; Ozaki, Y.; Suzuki, M.; Iwahashi, M. *Appl. Spectrosc.* **1998**, *52*, 994.
(23) Czarnecki, M. A. *J. Phys. Chem. A* **2000**, *104*, 6365.
(24) Czarnecki, M. A.; Orzechowski, K. *J. Phys. Chem. A* **2003**, *107*, 1119.
(25) Bourderon, C.; Peron, J. J.; Sandorfy, C. J. *J. Phys. Chem.* **1972**, *76*, 864.
(26) Yonker, C. R.; Wallen, S. L.; Palmer, B. J.; Garrett, B. C. *J. Phys. Chem. A* **1997**, *101*, 9564.
(27) Symons, M. C. R.; Robinson, H. L. *Phys. Chem. Chem. Phys.* **2001**, *3*, 535.
(28) Czarnecki, M. A.; Ozaki, Y. *Phys. Chem. Chem. Phys.* **1999**, *1*, 797.
(29) Czarnecki, M. A.; Czarnik-Matusewicz, B.; Ozaki, Y.; Iwahashi, M. *J. Phys. Chem. A* **2000**, *104*, 4906.
(30) Czarnecki, M. A. *J. Phys. Chem. A* **2003**, *107*, 1941.
(31) Iwamoto, R.; Matsuda, T.; Sasaki, T.; Kusanagi, H. *J. Phys. Chem. B* **2003**, *107*, 7976.
(32) Dixit, S.; Poon, W. C. K.; Crain, J. *J. Phys.: Condens. Matter* **2000**, *12*, L323.
(33) Sato, T.; Chiba, A.; Nozaki, R. *J. Mol. Liq.* **2002**, *101*, 99.
(34) Sassi, P.; Paolantoni, M.; Cataliotti, R. S.; Palombo, F.; Morresi, A. *J. Phys. Chem. B* **2004**, *108*, 19557.
(35) Gericke, A.; Gadaleta, S. J.; Brauner, J. W.; Mendelsohn, R. *Biospectroscopy* **1996**, *2*, 341.
(36) Czarnecki, M. A. *Appl. Spectrosc.* **1998**, *52*, 1583.
(37) Czarnecki, M. A. *Appl. Spectrosc.* **2000**, *54*, 986.
(38) Sato, T.; Chiba A.; Nozaki, R. *J. Chem. Phys.* **2000**, *112*, 2924.
(39) Czarnecki, M. A. *Appl. Spectrosc.* **1999**, *53*, 1392.
(40) D'Angelo, M.; Onori, G.; Santucci, A. *J. Chem. Phys.* **1994**, *100*, 3107.
(41) Zichi, D. A.; Rossky, P. J. *J. Chem. Phys.* **1986**, *84*, 2814.
(42) Iwahashi, M.; Suzuki, M.; Katayama, N.; Matsuzawa, H.; Czarnecki, M. A.; Ozaki, Y.; Wakisaka, A. *Appl. Spectrosc.* **2000**, *54*, 268.